sustainability

MDPI

Article

Experimental Investigations of the Hydrogen Injectors on the Combustion Characteristics and Performance of a Hydrogen Internal Combustion Engine

Min Huang [1], Qinghe Luo [1,2], Baigang Sun [1,2], Shiwei Zhang [1], Kangda Wang [1,2], Lingzhi Bao [1,*], Qian Li [3,4], Xuelin Tang [3] and Wei Deng [3]

[1] School of Mechanical Engineering, Beijing Institute of Technology, Beijing 100081, China; 3120210469@bit.edu.cn (M.H.); luoqinghe@bit.edu.cn (Q.L.); bitzhangshiwei@163.com (S.Z.); 13520315912@163.com (K.W.)
[2] Beijing Institute of Technology Chongqing Innovation Center, Chongqing 401121, China
[3] New Powertrain R&D Institute, Chongqing Changan Automobile Co., Ltd., Chongqing 401133, China
[4] College of Mechanical and Vehicle Engineering, Chongqing University, Chongqing 400030, China
* Correspondence: lingzhibao@bit.edu.cn

Abstract: Hydrogen is regarded as an ideal zero-carbon fuel for an internal combustion engine. However, the low mass flow rate of the hydrogen injector and the low volume heat value of the hydrogen strongly restrict the enhancement of the hydrogen engine performance. This experimental study compared the effects of single-injectors and double-injectors on the engine performance, combustion pressure, heat release rate, and the coefficient of variation (CoV_{IMEP}) based on a single-cylinder 0.5 L port fuel injection hydrogen engine. The results indicated that the number of hydrogen injectors significantly influences the engine performance. The maximum brake power is improved from 4.3 kW to 6.12 kW when adding the injector. The test demonstrates that the utilization of the double-injector leads to a reduction in hydrogen obstruction in the intake manifold, consequently minimizing the pumping losses. The pump mean effective pressure decreased from −0.049 MPa in the single-injector condition to −0.029 MPa in the double-injector condition with the medium loads. Furthermore, the double-injector exhibits excellent performance in reducing the coefficient of variation. The maximum CoV_{IMEP} decreased from 2.18% in the single-injector configuration to 1.92% in the double-injector configuration. This result provides new insights for optimizing hydrogen engine injector design and optimizing the combustion process.

Keywords: hydrogen internal combustion engine; hydrogen injector; engine performance; combustion characteristics; coefficient of variation

Citation: Huang, M.; Luo, Q.; Sun, B.; Zhang, S.; Wang, K.; Bao, L.; Li, Q.; Tang, X.; Deng, W. Experimental Investigations of the Hydrogen Injectors on the Combustion Characteristics and Performance of a Hydrogen Internal Combustion Engine. *Sustainability* **2024**, *16*, 1940. https://doi.org/10.3390/su16051940

Academic Editor: Elena Cristina Rada

Received: 18 January 2024
Revised: 21 February 2024
Accepted: 22 February 2024
Published: 27 February 2024

1. Introduction

According to statistics from the International Energy Agency, non-renewable energy sources such as oil, coal [1], and natural gas remain the predominant sources of energy consumption, and their consumption continues to grow [2,3]. This not only gives rise to environmental issues such as global warming [4,5] but also leads to problems related to energy shortages [6,7]. In response to these challenges and increasingly stringent environmental regulations, new energy vehicles [8], fuel cell vehicles [9], and hybrid vehicles [10] have been introduced to the market. However, these new technologies come with issues, such as battery fires, high manufacturing costs, and carbon emissions concerns. Therefore, in the short term, internal combustion engines continue to be the primary source of propulsion [11]. In response to energy shortages [12] and climate change, researchers are actively searching for renewable and clean energy sources, such as natural gas [13], hydrogen [14], biofuels [15], and ethanol [16].

Hydrogen is one of the most promising zero-carbon fuels and it is the best alternative to fossil fuels [17]. As a clean and renewable fuel, hydrogen has many advantages, including

a high calorific value [18], wide sources, and zero pollution. It is considered to be an important energy carrier for the future [19,20]. Hydrogen internal combustion engines have broad prospects in the field of hydrogen energy utilization [21]. Hydrogen can be directly used in traditional internal combustion engines without the need for significant modifications to conventional internal combustion engines. According to the fuel injection method, hydrogen internal combustion engines can be divided into port fuel injection (PFI) and direct injection (DI) internal combustion engines [22]. While hydrogen direct injection in the cylinder requires a high injection pressure, the lubrication problem of the hydrogen injector is difficult to solve. Therefore, port fuel injection is currently the best choice due to its simple structure and easy implementation advantages.

The characteristics of hydrogen are a fast burning speed [23], low ignition energy [24], short quenching distance [25], and wide combustion limit. Many scholars have demonstrated that the use of hydrogen can improve the indicated thermal efficiency of internal combustion engines and reduce HC and CO emissions [17,26,27]. However, due to the extremely low volumetric density of hydrogen, hydrogen internal combustion engines still have the disadvantage of a low power density. With the development of hydrogen internal combustion engines, hydrogen injectors have gradually become a key factor in improving the performance of hydrogen internal combustion engines.

As we all know, the injector plays a key role in the hydrogen internal combustion engine. It determines the method, timing, and location of fuel injection, directly affecting the efficiency and characteristics of the combustion process. Therefore, the injector has a significant impact on the performance and emissions of hydrogen internal combustion engines. In recent years, the research concerning the effect of hydrogen injectors on engine performance has gradually increased. One important research direction is to explore the influence of single-injector and double-injector configurations on hydrogen combustion engine performance.

A. Cernat [28] and his colleagues conducted experiments on the combustion of hydrogen in diesel engines and found that the maximum pressure rise rate was increased after the addition of hydrogen, and NOx and smoke were also reduced. Nurullah Gültekin [29] and his team conducted experiments on a single-cylinder hydrogen–diesel dual-fuel engine. The results indicated that the addition of hydrogen increased the peak combustion pressure and reduced emissions of HC and CO. However, there was a significant increase in NOx emissions. Taku Tsujimura et al. [30] pointed out that the low-pressure injection of hydrogen affects the mixing rate of hydrogen and air, resulting in increased emissions. Murat Ciniviz et al. [29] conducted experiments on a single-cylinder diesel engine. The study found that when diesel is mixed with hydrogen, it increases the combustion pressure and reduces the specific energy consumption. Also, the study found that there was an increase in NO emissions and a significant decrease in other emissions. Kubilay Bayramoğlu et al. [31] researched the single-cylinder, four-stroke diesel engines. They found that increasing the hydrogen blending ratio and advancing the hydrogen injection timing greatly improved the engine power, thermal efficiency, and IMEP. However, it also increased NOx emissions. Sadashiva Lalsangi [32] and his team indicated that optimizing the hydrogen injection timing and hydrogen injection pulse width can reduce CO emissions and improve thermal efficiency. Xinyu Liu [33] and colleagues observed the following phenomenon through their experiments. The hydrogen injection timing directly influenced the formation and combustion of the mixture. After adding hydrogen to a single-cylinder diesel engine, the engine's indicated thermal efficiency (ITE) reached 57.2%. Liu, CY [34] and his research group obtained the following conclusions through experiments. Compared with multiple injectors, a single nozzle has a larger jet penetration depth and a larger combustion release rate. However, the combustion efficiency is lower. Chen Pu [35] and colleagues used an injector with dual orifices to inject hydrogen and then investigated the effects of different jet schemes on the mixture formation. They found that the injection angle and direction between the two orifices affected the mixture formation.

Javad Zareei [36] and his team researched a PFI engine. They found that increasing the number of injector orifices can improve the engine performance and reduce emissions.

In conclusion, the number of injectors has a significant impact on the performance of hydrogen internal combustion engines. However, the effect of the injector number on the PFI hydrogen engine's performance has been poorly studied. Therefore, it is necessary to carry out relevant experimental studies to explore the influence of injector numbers on the PFI hydrogen internal combustion engine's performance. Then, researches are to fill the gaps in this field. In this research, the same engine was equipped with both single-injector and double-injector conditions, and their effects on the combustion process and performance of the PFI hydrogen internal combustion engines were investigated. This research will provide a new method for optimizing the performance of PFI single-cylinder hydrogen internal combustion engines.

2. Experimental Setup

2.1. Engine Testing Platform

The hydrogen injector is the core component of the hydrogen internal combustion engine, and through calculation and analysis, the hydrogen injector of the American Quantum Company was selected. It has the advantage of a fast response and long service life. The actual injector is shown in Figure 1, and its main technical parameters are listed in Table 1.

Figure 1. Hydrogen injector.

Table 1. Hydrogen Injector Technical Parameters.

Parameter	Value
Operating voltage/V	8~16
Driving current/A	Peak 4 A/Hold 1 A
Work pressure/bar	1.03~5.52
Hydrogen flow/g/s	0.8@5.52 bar
Resistance/Ω	2.05@20 °C
Inductance/mH	3.98@1000 Hz

The flow characteristics of the hydrogen injector are shown in Figure 2, which shows the variation of the flow rate of the hydrogen injector with the pulse width of the injection under different injection pressures. It can be seen that the flow rate of the hydrogen injector increases linearly with the injection pulse width.

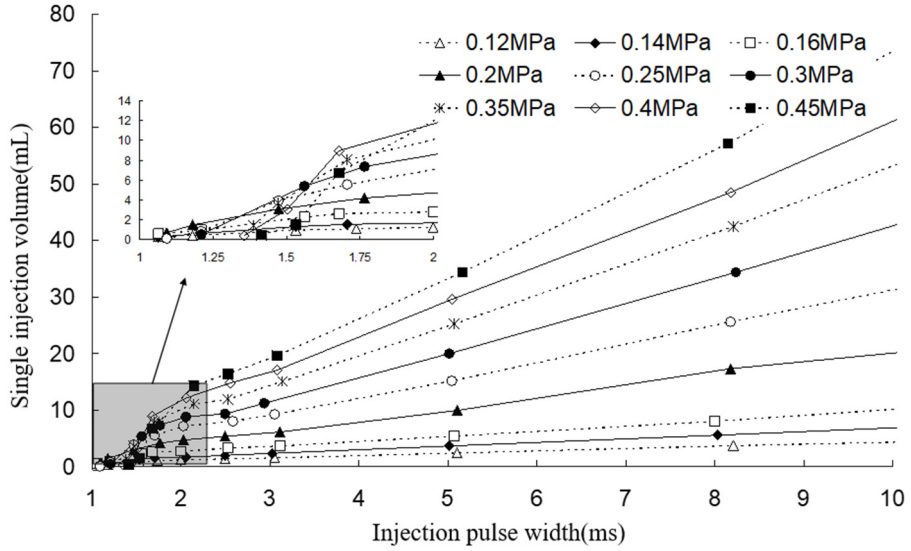

Figure 2. The variation in the injector flow rate with the injection pulse width at different injection pressures.

The response characteristics of the hydrogen injector are shown in Figure 3. It shows the driving current signal during hydrogen injection. The hydrogen pressure changes in the hydrogen supply pipeline at the front end of the injector, and the hydrogen pressure changes at the back end of the injector when the injection pressure is 0.4 MPa and the injection pulse width is 10 ms. As the injector driving current gradually increases from 0 to about 4 A, the injector is turned on at t0 time, and the hydrogen pressure at the front of the injector decreases rapidly. At the same time, the driving current is reduced to 1 A to keep the injector fully open. With the end of the hydrogen injection process, the injector driving current gradually decreases to 0, the injector is gradually closed at this time, and the hydrogen injection process ends.

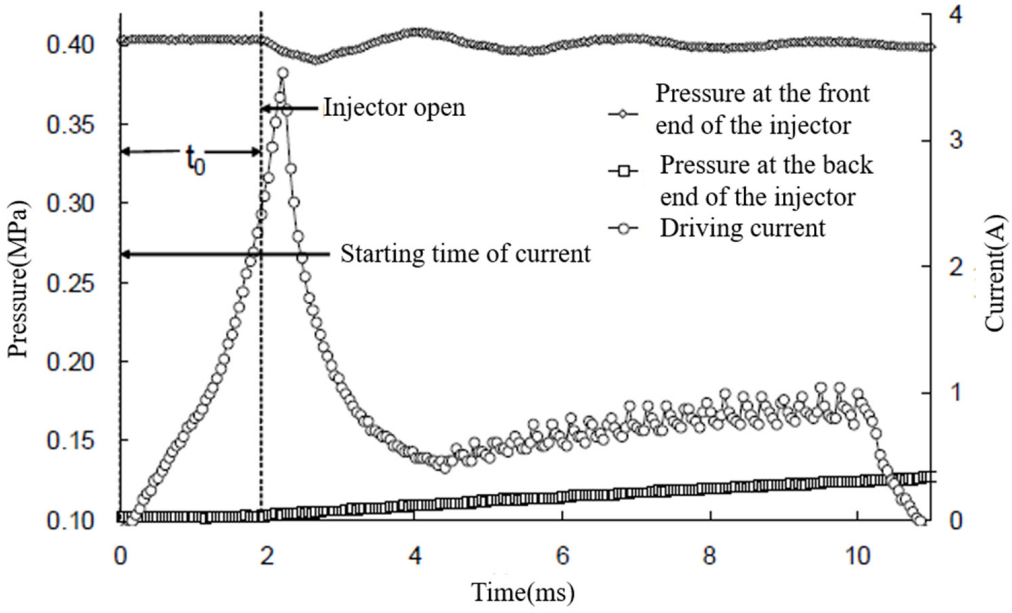

Figure 3. Variation in the hydrogen supply pressure, back pressure, and driving current during hydrogen injection.

The test engine is a four-stroke, two-valve, 0.5 L displacement single-cylinder engine with spark plug ignition. The combustion structure is a spherical combustion chamber, and the fuel injection method is PFI. The original engine is a gasoline engine. Its intake manifold and fuel supply system were modified to become a hydrogen internal combustion engine. Figure 4 illustrates the physical structure of the single-injector and double-injector. The specific parameters of the experimental engine are presented in Table 2.

(**a**) single-injector (**b**) double-injector

Figure 4. Schematic of the single-injector and double-injector structure.

Table 2. The Main Parameters of the Engine.

Parameters	Value
Number of Cylinders	1
Intake Method	Naturally Aspirated
Fuel Supply Method	PFI
Bore/mm	92
Stroke/mm	69
Connecting Rod Length/mm	112.3
Compression Ratio	8.4
Displacement/L	0.458

Figure 5 shows a schematic diagram of the engine test bench. During the experiment, a 15 MPa hydrogen tank was used to provide hydrogen. The purity of the hydrogen is 99.99%. After the hydrogen passes through the primary pressure reducing valve and the secondary pressure reducing valve, the pressure is reduced to 3.5 MPa to avoid damage to the injector. The dynamometer of the test bench is Power-Link's GW10 (Xiangyi and Changsha, China), which is used to measure the engine power and torque. The control system of the engine bench is the FC2000 engine measurement and control system (Xiangyi and Changsha, China).

The air flow rate was measured by the precession vortex flowmeter. The hydrogen flow rate was measured by the seven-star volumetric flow meter. Additionally, to reduce the fluctuation of the intake pressure, a large-volume stabilizer box was added to the air inlet to stabilize the air pressure.

AVL's Kibox combustion analyzer (Kistler and Shanghai, China) was utilized to collect data such as the combustion pressure, heat release rate, and more. Kistler's spark plug-style cylinder pressure sensor (Kistler and Shanghai, China) was used to measure the combustion pressure in the cylinder. An angle encoder was used to measure the engine's crankshaft speed. The PT100 sensors were used to monitor the coolant and oil temperature. Communication with the ECU was established through an upper computer. The MotoHawk software (ECM-0554-112-0904-C/F) was used to configure test parameters such as the

ignition timing, hydrogen injection timing, and injection pulse width. The parameters of the equipment used in the experiment are detailed in Table 3.

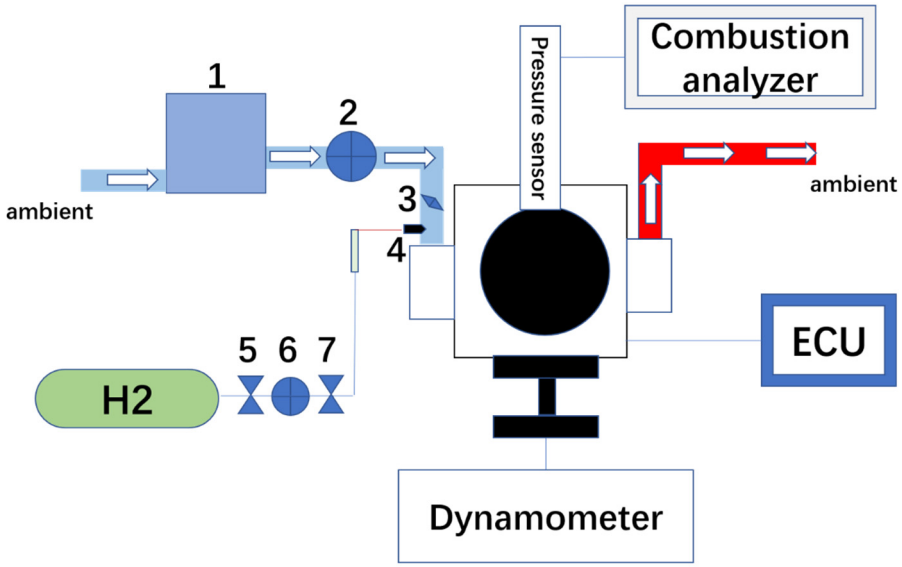

Figure 5. Schematic Diagram of the Engine Test Stand.

Table 3. Main Experimental Equipment.

Parameters	Model	Accuracy
Engine Speed	GW10	±1 rpm
Torque	GW10	±0.24 N·m
Air Flow Rate	Vortex flowmeter	±0.3 m^3/h
Hydrogen Flow Rate	Seven-star Volumetric Flowmeter	±0.5 cm^3/min
Combustion Pressure	Kistler 6052C transducer	±0.02 MPa

2.2. Experimental Procedure

During the experiment, the experimental process should be documented in detail, which can reduce the experimental error and make the experiment reproducible. First, the pressure of the hydrogen tank is as high as 15 MPa, and the pressure reducing valve is adjusted to reduce the hydrogen pressure to 3.5 MPa while keeping the hydrogen injection pressure constant, and then the hydrogen is injected into the cylinder through the injector. Second, during the experiment, the dynamometer is set to n/P gear to ensure that the dynamometer can adjust the engine speed. The engine speed is controlled by the dynamometer, which is gradually increased from 1500 rpm to 4500 rpm at intervals of 500 rpm. The engine load is controlled by the pulse width of hydrogen injection, and the BMEP gradually increases from 0.15 to 0.45 MPa, with an interval of 0.05 MPa. At the same time, during the experiment, the intake air temperature was maintained at 25 °C and the oil temperature was maintained at 85 °C. This is to ensure that the variables are unique.

The experiment is to compare the effect of the single-injector and double-injector on the engine performance. The working conditions of the test process include the engine speed range of 1500 to 4000 rpm and the BMEP range of 0.15 to 0.45 MPa.

During the experiments, the engine was left to run for a while after starting it. When the oil and coolant temperature reached the appropriate value, the engine speed, ignition timing, hydrogen injection pulse width, and other parameters were adjusted. Data

recording began as soon as the target condition was reached. To reduce the test error, the 210 cycles of data were recorded each time and then averaged.

In the performance comparison experiment of the single-injector and double-injector, the maximum power, torque, and BMEP in the engine speed change range of 1500~4500 rpm were tested and recorded. In the comparative experiments of combustion characteristics under the single-injector and double-injector conditions, experiments were conducted at a constant engine speed of 3000 rpm and with BMEP ranging from 0.25 to 0.35 MPa. Combustion-related data such as the cylinder pressure and heat release rate were recorded. Finally, in the comparison experiment of the engine cycle variation, IMEP and CoV_{IMEP} under different working conditions with an engine speed of 2500~3500 rpm and BMEP of 0.25~0.35 MPa were tested and recorded.

During the whole experimental process, CoV_{IMEP} was controlled within 5% to avoid severe engine vibration affecting the accuracy of the experiment process.

3. Results and Discussion

3.1. Performance Comparison of the Single-Injector and Double-Injector

Under the premise of avoiding abnormal combustion such as backfire and knock, a comparative study was conducted with the single-injector and double-injector. The maximum power, torque, and BMEP that the engine can achieve at different speeds are explored.

As shown in Figure 6, the power comparison chart illustrates the performance of the single-injector and double-injector at different engine speeds. The power of the single-injector first increases and then decreases with the increase in the engine speed, reaching a maximum of 4.3 kW at 3000 rpm and only 3.1 kW at 4000 rpm, a decrease of 26.1%. In contrast, with the double-injector, the engine's power consistently increases with the engine speed, reaching 6.12 kW at 4000 rpm. Because the engine speed is higher, the engine does more work per unit time. Thus, the engine power is greater. However, when the speed reaches 3000 rpm, the injection capacity of the single-injector is insufficient, resulting in the air–fuel mixture being too lean. Therefore, the CoV_{IMEP} in the cylinder is increased, and the combustion is unstable. Thereby, the throttle opening can only be reduced, so the power decreases.

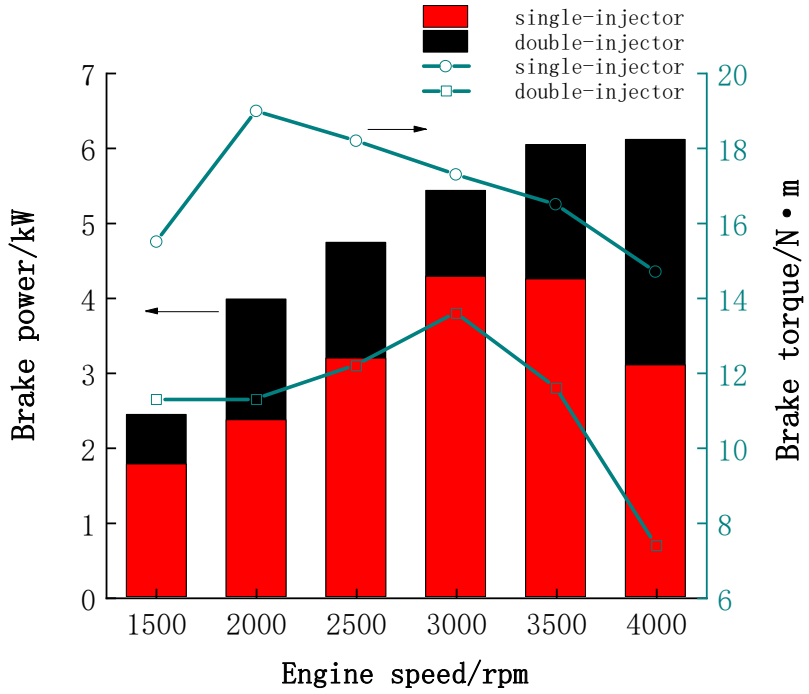

Figure 6. Comparison of maximum power and torque at different speeds.

Furthermore, the minimum and maximum torque of the single-injector condition are 7.4 N·m and 13.6 N·m, respectively. In contrast, under the double-injector condition, the minimum torque is 14.5 N·m and the maximum torque is 19.0 N·m. Therefore, the engine torque characteristics at the double-injector are better than those at the single-injector.

Figure 7 shows the comparison of the air mass flow rate of the single-injector and double-injector at different speeds. It can be seen that as the speed increases, the air mass flow rate continues to increase, because as the speed increases, the engine's air intake increases per unit time. In addition, the air mass flow rate in the double-injector condition is significantly greater than that in the single-injector condition. The maximum air mass flow rate in the single-injector and double-injector working conditions is 0.0092 kg/s and 0.0102 kg/s, respectively. Hydrogen "clogs" the intake manifold, making the air mass flow rate from the single-injector smaller than that with the double-injector configuration. There are several reasons for the phenomenon of "blockage": first, the molecular mass of hydrogen is very small, hydrogen is a gas, and the hydrogen expands rapidly after being injected into the intake manifold, resulting in a decrease in the effective circulation area of the air, which reduces the intake air mass; second, the pulse width of the hydrogen injection is a specific period of time, generally a few milliseconds, during which the hydrogen is continuously injected into the intake manifold and stays in the intake manifold. As a result, the "blockage" effect of hydrogen affects the air flow in the intake duct. However, under the condition of a double-injector, the hydrogen injection time is greatly shortened, the residence time of hydrogen in the intake manifold is shortened, and the "blockage" effect of hydrogen is significantly reduced, so the air mass flow into the cylinder is larger.

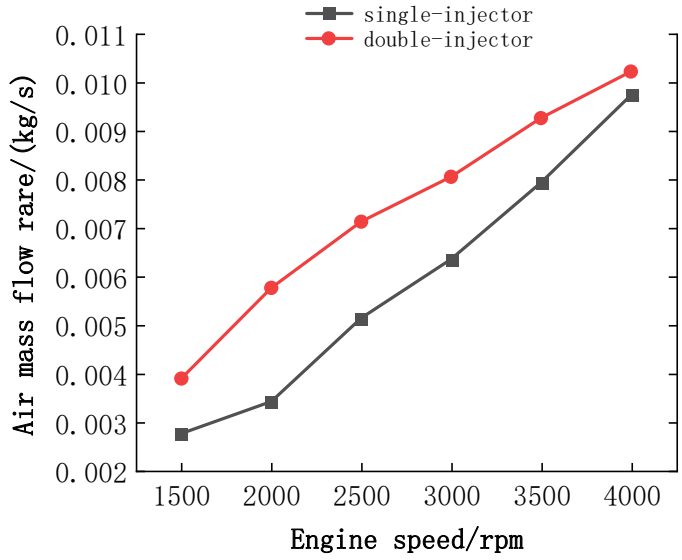

Figure 7. Variation in the air mass flow rate at different speeds.

Gao, Jianbing [37], and Bifen Wu [38] pointed out that the PFI hydrogen internal combustion engine will cause the backfire phenomenon and reduce the engine performance at the same time. Similarly, the phenomenon of backfire also occurred during the experiment. Figure 8 shows a comparison of the excess air coefficient at 2000 rpm for the single-injector and double-injector. From the figure, it can be seen that the λ change range of the single-injector configuration is 1.70~2.47. However, the excess air coefficient of the double-injector condition has a larger variation range, which is 1.49~2.97. Furthermore, when the excess air coefficient is equal, the power of the double-injector condition is greater than the power of the single-injector condition. Because of the limited injection capacity of the single-injector, the amount of hydrogen injection is small. Thus, the power of the single-injector working condition is less than that of the double-injector condition. Limited by the insufficient injection capacity of the single-injector, the λ minimum value is 1.70. Therefore, it can be known

that the injection boundary of the double-injector is larger than that of the single-injector. In addition, under the single-injector condition, when the excess air coefficient reaches around 2.5, the engine vibrates due to the unstable combustion. Limited by abnormal combustion, the mixture cannot be too lean, so λ cannot continue to increase. In contrast, the combustion is relatively stable under the double-injector condition. So, the excess air coefficient λ can be increased to 2.97. This is because the intake manifold is blocked by hydrogen under the single-injector conditions, which worsens the scavenging process. Consequently, there is less fresh air entering the cylinder, so there is more residual exhaust gas in the cylinder, which increases the likelihood of abnormal combustion. Therefore, the lean combustion boundary of the double-injector is also greater than that of the single-injector condition.

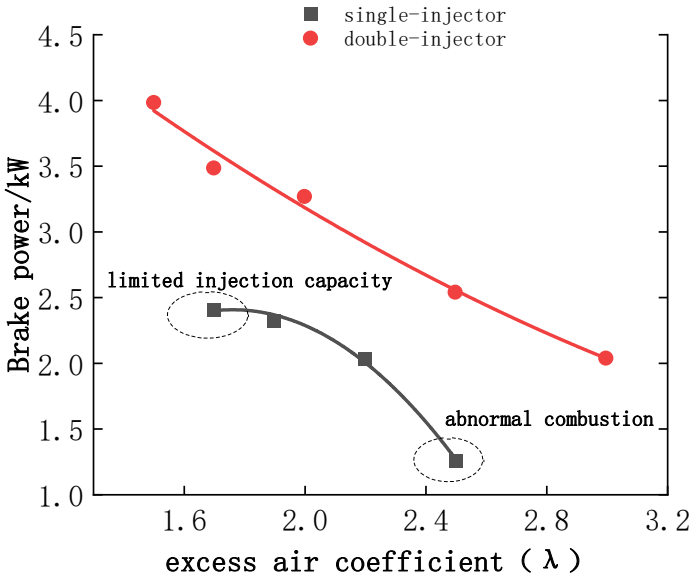

Figure 8. Variation in output power at different air–fuel equivalence ratios.

Figure 9 shows a comparison chart of the PMEP. As can be seen from the figure, the PMEP of both the single-injector and double-injector is negative, and the PMEP of the double-injector is smaller than that of the single-injector.

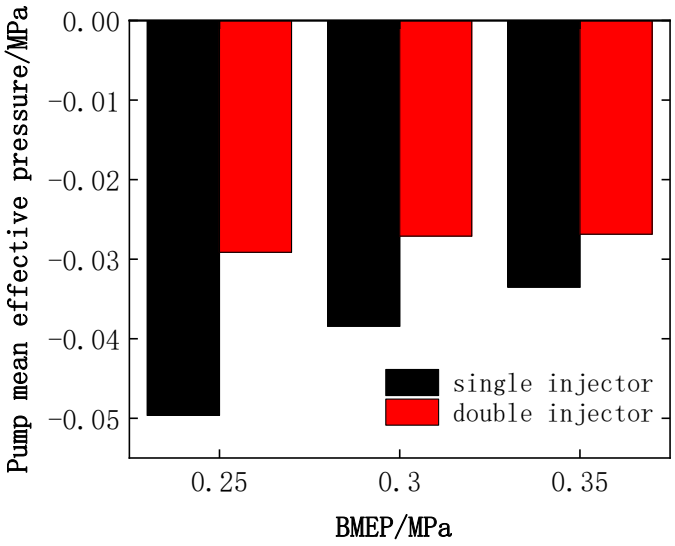

Figure 9. Comparison of PMEP under different loads.

When the BMEP is 0.35 MPa, the PMEP of the single-injector and double-injector is −0.034 MPa and −0.027 MPa, respectively. This shows that under the single-injector condition, the engine's scavenging process is worse, and the pumping loss is greater. This is because the "blockage" phenomenon of hydrogen in the intake manifold under the single-injector condition is more obvious, and the "blockage" effect is weaker under the double-injector condition. Hence, in the double-injector condition, hydrogen and fresh air can enter the cylinder more smoothly, and the airflow movement in the cylinder is better. Therefore, the PMEP in the double-injector is smaller.

In addition, the double-injector increases the intake air mass, enhances the scavenging effect, and reduces the residual exhaust gas in the cylinder. Consequently, this not only improves the volumetric efficiency and reduces the maximum temperature in the cylinder but also reduces the occurrence of abnormal combustion and improves the engine performance. It also shows that the abnormal combustion boundary of the double-injector is larger than that of the single-injector.

3.2. Combustion Characteristics of the Single-Injector and Double-Injector

Since the combustion characteristics of other speeds and loads are the same, this analysis focuses on the combustion characteristics of the single-injector and double-injector at the maximum power point with an engine speed of 2500~3500 rpm and a BMEP of 0.25~0.35 MPa, with an engine speed of 3000 rpm.

Figure 10 illustrates the change curve of the combustion pressure of the single-injector and double-injector with the crankshaft angle under different loads and different speeds. It can be seen that at the maximum power point of 3000 rpm, the maximum combustion pressure of the single-injector and double-injector working conditions is 2.64 MPa and 3.61 MPa, respectively. When the BMEP is 0.30 MPa, the maximum combustion pressure of the single-injector and double-injector is 2.84 MPa and 2.89 MPa, respectively. At the same load condition, the combustion pressure of the double-injector condition is greater than the combustion pressure of the single-injector condition. At the maximum power point, the phenomenon is similar to the above. This is because the double-injector can shorten the hydrogen injection time, and hydrogen can enter the cylinder faster, alleviating the "blockage" phenomenon in the intake manifold. Thereby, the air quality entering the cylinder under the double-injector condition is more than that in the single-injector condition. Due to the increase in the working fluid in the cylinder, the combustion pressure in the cylinder of the double-injector is greater than that of the single-injector during the combustion process.

Figure 11a shows the max combustion pressure and Figure 11b shows the maximum pressure rise rate of the single-injector and double-injector under different working conditions. From Figure 11a, it is obvious that under different working conditions, the maximum combustion pressure of the double-injector configuration is almost greater than that of the single-injector setup. From the diagram, we can see that at the maximum power point of 2500 rpm, the maximum combustion pressures of the single-injector and double-injector working conditions are 3.17 MPa and 4.06 MPa, respectively. At the BMEP of 0.25 MPa, the maximum combustion pressures of the single-injector and double-injector are 2.45 MPa and 2.47 MPa. Because in the double-injector configuration, the air intake volume is larger, there is more working fluid, so the maximum combustion pressure is correspondingly larger.

However, the trend of the maximum pressure rise rate is not the same in Figure 11b. At 2500 rpm, the maximum power of the single-injector and double-injector is 3.19 kW and 4.74 kW, respectively. At the maximum power point of 2500 rpm, the maximum pressure rise rate for the double-injector case is 0.213 MPa/°CA, which is significantly greater than the 0.208 MPa/°CA for the single-injector condition. The reason for this phenomenon is that the power is greater and more hydrogen is injected. As a result, the burning rate in the cylinder is faster, so the pressure rise rate increases. The change trends in the pressure rise rate of other speed conditions are similar. At 3000 rpm and a BMEP of 0.30 MPa, the maximum pressure rise rates of the single-injector and double-injector are 0.174 MPa/°CA

and 0.079 MPa/°CA, respectively. Also, it can be seen that with the increase in BMEP, the maximum pressure rise rate increases. This is because as the load increases, more hydrogen enters the cylinder, and the burning rate is faster, so the pressure rise rate will also increase. In addition, under the same load conditions, it is obvious that the pressure rise rate of the single-injector is greater than that of the double-injector. Because the combustion in the cylinder of the double-injector is more stable, the ignition timing is more advanced. In contrast, the working condition of the single-injector is unstable and the ignition timing is relatively delayed. The ignition timing of the single-injector is backward, and thanks to the fast flame propagation speed of hydrogen, the mixture burns rapidly near the top dead center. Therefore, it is closer to constant-volume combustion, and the pressure rise rate is larger.

Figure 12 is a trend chart of the heat release rate. At the maximum power point of the same speed, the peak heat release rate of the double-injector is greater than that of the single-injector. This phenomenon is mainly because the double-injector provides more hydrogen at the maximum power point, so the burning rate and heat release rate in the cylinder are faster. However, under the same load conditions, the instantaneous heat release rate curve of the double-injector is relatively smooth, and the combustion starts early and ends late. From the figure, the heat release of the double-injector configuration starts at about −15 °CA and lasts to 40 °CA, peaking at 8 °CA. In the case of the single injector setup, the heat release curve is steep and the heat release is more concentrated. The heat release starts from −10 °CA and lasts to 20 °CA. Because the combustion in the cylinder of the single-injector condition is unstable, the ignition timing is delayed, so the starting point of combustion and heat release in the single-injector condition is backward.

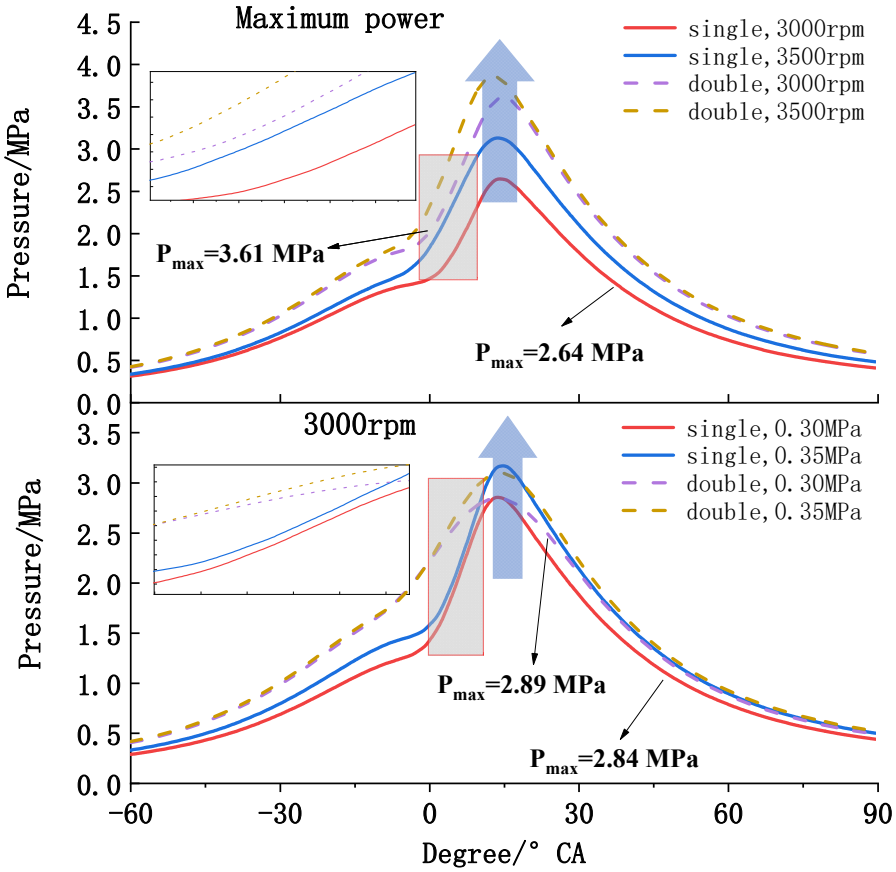

Figure 10. Comparison of the combustion pressure at different operating conditions.

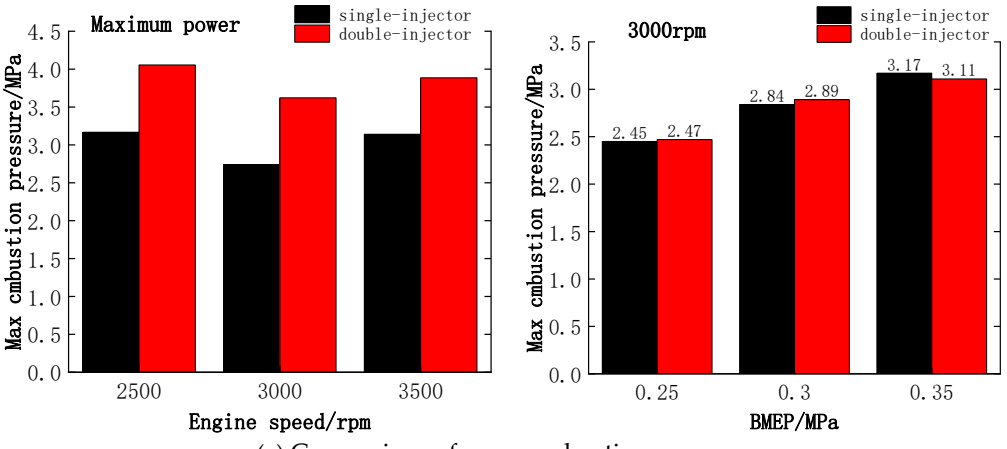

(**a**) Comparison of max combustion pressure

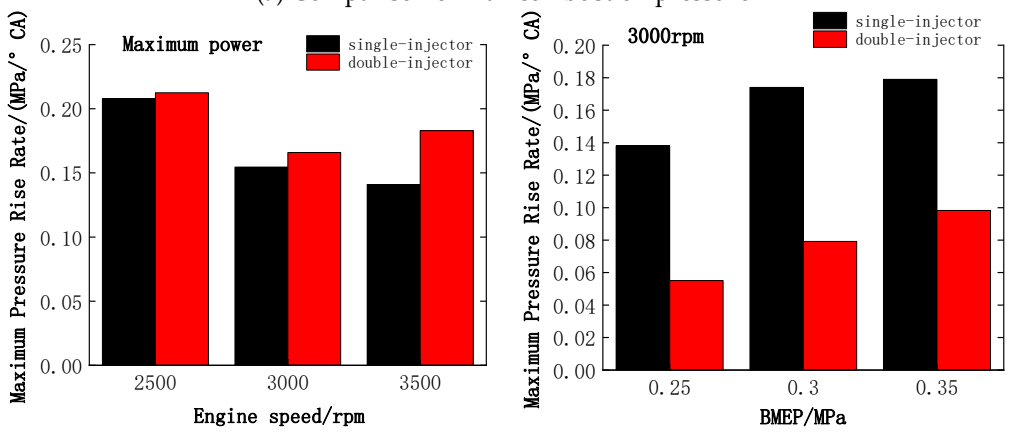

(**b**) Comparison of maximum pressure rise rate

Figure 11. Comparison of the Max Combustion Pressure and Maximum Pressure Rise Rate at Different Working Conditions.

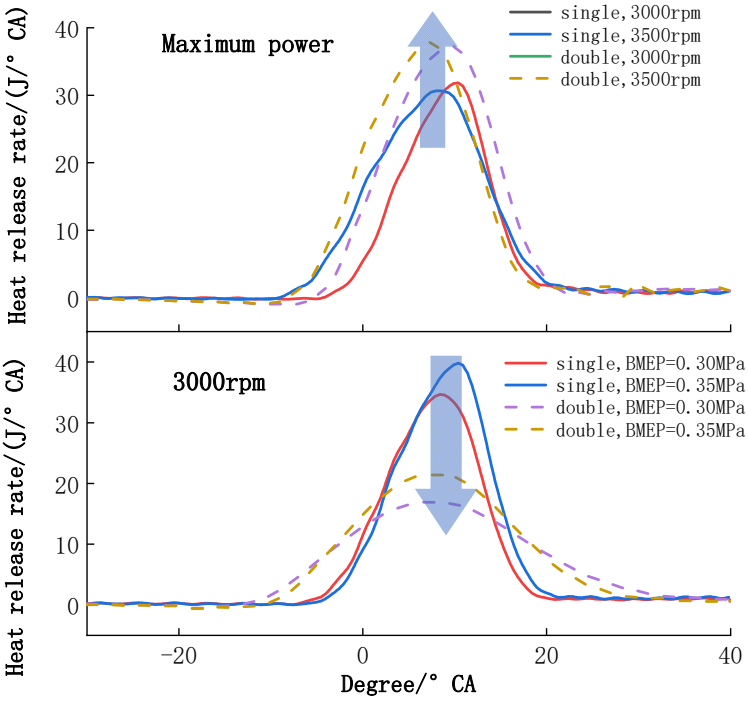

Figure 12. Comparison of Combustion Heat Release Rates under Different Loads.

Figure 13 shows a comparison of the maximum heat release rate of the single-injector and double-injector configurations. From Figure 13a, at the maximum power point of 2500 rpm, the maximum heat release rates of the single-injector and double-injector configurations are 42.90 J/°CA and 49.85 J/°CA, respectively. The principle is similar to the analysis in the previous paragraph. On the contrary, from Figure 13b, when the BMEP is 0.30 MPa, the maximum heat release rates of the single-injector and double-injector are 37.72 J/°CA and 17.88 J/°CA, respectively. As previously explained in Section 2.1, when reaching the same load condition, the excess air coefficient of the double-injector condition is larger. It means that more air in the mixture does not participate in the reaction. Therefore, compared with the single-injector condition, the concentration of the mixture in the double-injector condition is lower, and the propagation speed of the flame is reduced. The heat release rate of the double-injector condition is smaller than that of the single-injector condition. However, it is worth noting that a large pressure rise rate and heat release rate will increase the deflagration tendency of the engine.

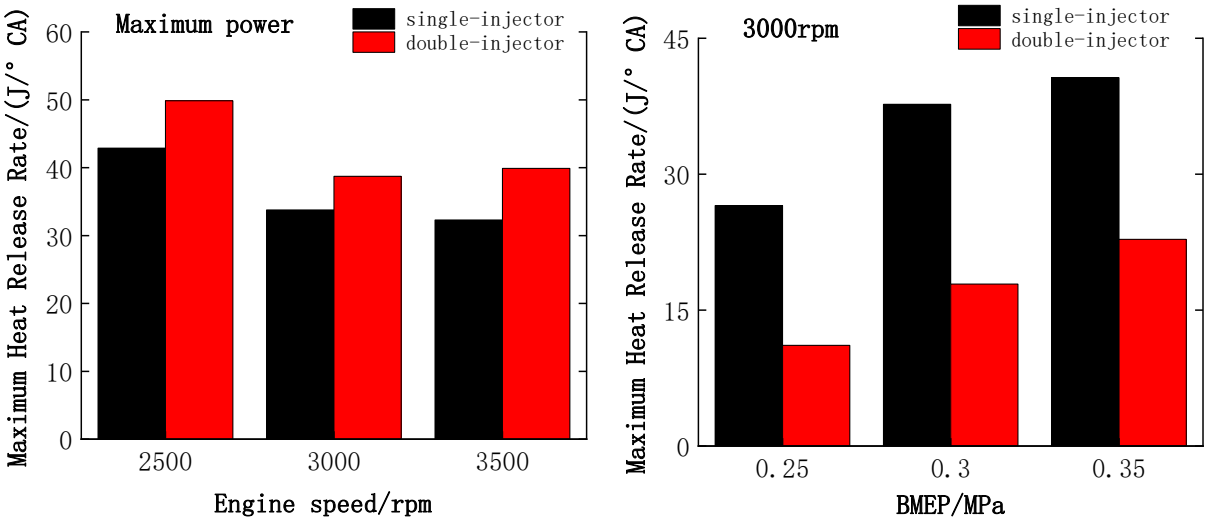

(**a**) At the maximum power point (**b**) At 3000 rpm

Figure 13. Comparison of Maximum Heat Release Rates under Different Conditions.

In summary, under the same load conditions, the double-injector configuration can increase the fresh air entering the cylinder and reduce the concentration of the mixture. Therefore, the burning rate of the mixture is reduced, and the pressure rise rate and instantaneous heat release rate of the double-injector condition are smaller, which effectively reduces the mechanical load and thermal load of the engine.

Figure 14 is the indicated thermal efficiency comparison of the single-injector and double-injector. From Figure 14a, at the maximum power point of 3000 rpm, the ITE of the single-injector and double-injector is 22.69% and 35.12%, respectively. From Figure 14b, at a BMEP of 0.30 MPa, the ITE of the single-injector and double-injector is 30.45% and 34.01%, respectively. Notably, the ITE of the double-injector is greater than that of the single-injector configuration. The main reasons are as follows. First of all, the double-injector has a shorter fuel injection duration. So, the hydrogen–air mixing time is longer, the mixture uniformity is better, and the combustion is more stable. Second, due to the greater instantaneous heat release rate of the single-injector condition, the heat transfer loss is increased. Furthermore, the pumping loss is smaller in the double-injector configuration. In summary, compared to the single-injector configuration, the ITE of the double-injector is higher.

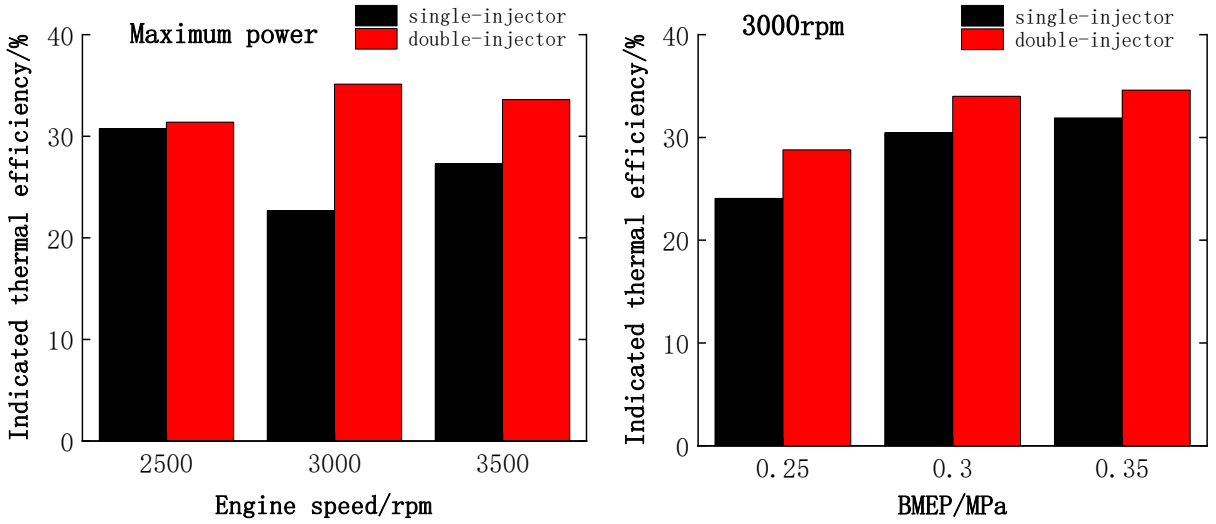

(**a**) At the maximum power point (**b**) At 3000 rpm

Figure 14. Efficiency Comparison Under Different Operating Conditions.

Figure 15 is a comparative chart of the burning duration between the single-injector and double-injector. As shown in Figure 15a, at 2500 rpm, the burning duration of the single-injector and double-injector is 26.19 °CA and 27.15 °CA, respectively. At the maximum power point, the burning duration of the double-injector is greater than that of the single-injector. Because the double-injector configuration has more of the air–fuel mixture in the cylinder, it leads to an increase in the burning duration. In addition, it can be seen that under the same load conditions, the burning duration of the double-injector is also longer than that of the single-injector. As depicted in Figure 15b, at a BMEP of 0.30 MPa, the burning duration of the single-injector and double-injector is 16.04 °CA and 29.35 °CA, respectively. The reasons for this phenomenon are as follows. Under the single-injector condition, the blocking phenomenon of hydrogen gas on the intake manifold is more obvious, and it takes longer for hydrogen to enter the cylinder. When the intake valve is closed, the concentration of hydrogen near the spark plug is higher, so the mixture burns faster after the spark ignition. Conversely, the excess air coefficient of the double-injector condition is larger, and the burning rate is slower. Correspondingly, the burning duration is longer.

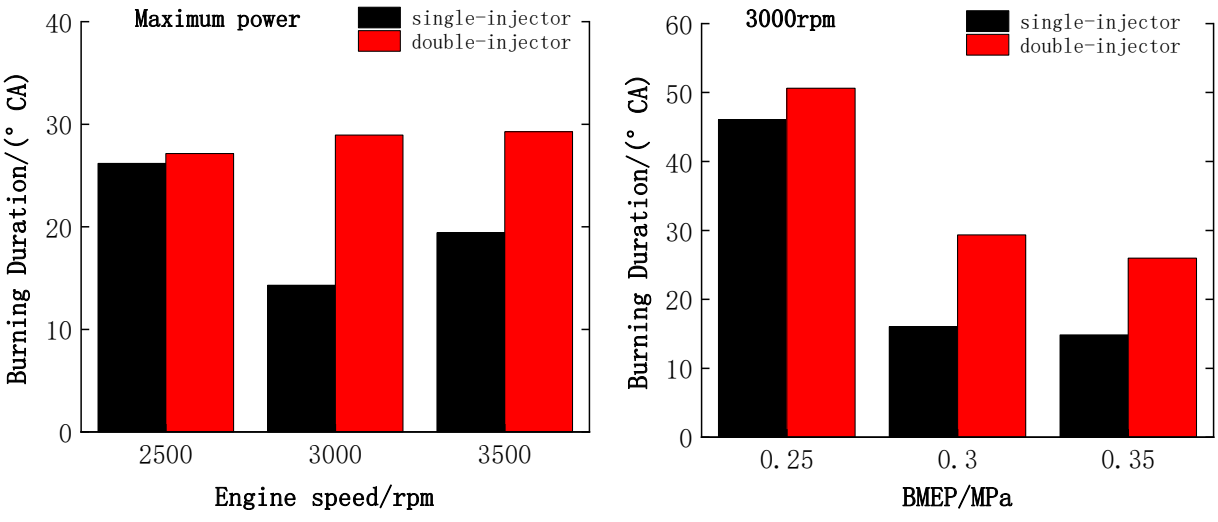

(**a**) At the maximum power point (**b**) At 3000 rpm

Figure 15. Comparison of Burning Durations under Different Operating Conditions.

3.3. Comparison of CoV_{IMEP}

CoV_{IMEP} is an important parameter for evaluating the working process of a hydrogen internal combustion engine. Yu, Xiumin et al. [39] found that hydrogen blending with gasoline could reduce the CoV_{IMEP} of combustion. Also, Jayashish Kumar Pandey [40] found that hydrogen blending with butanol could reduce the CoV_{IMEP}. There has been a lot of research on dual-fuel internal combustion engines. However, the CoV_{IMEP} of pure hydrogen internal combustion engines has been less studied.

In order to compare the influence of a single-injector and double-injector on the CoV_{IMEP}, the experimental conditions were set at 3000 rpm, the BMEP was set to 0.25~0.35 MPa, and the ignition timing was the maximum brake torque (MBT) ignition timing. As shown in Figure 16, it can be seen that under the same load, the IMEP fluctuation of the single-injector condition is larger than that of the double-injector, and the fluctuation of IMEP becomes smaller with the increase in the load. Figure 17 illustrates the characteristic curve of the CoV_{IMEP} with the load. Notably, it can be found that the CoV_{IMEP} of the single-injector working condition is greater than that of the double-injector condition.

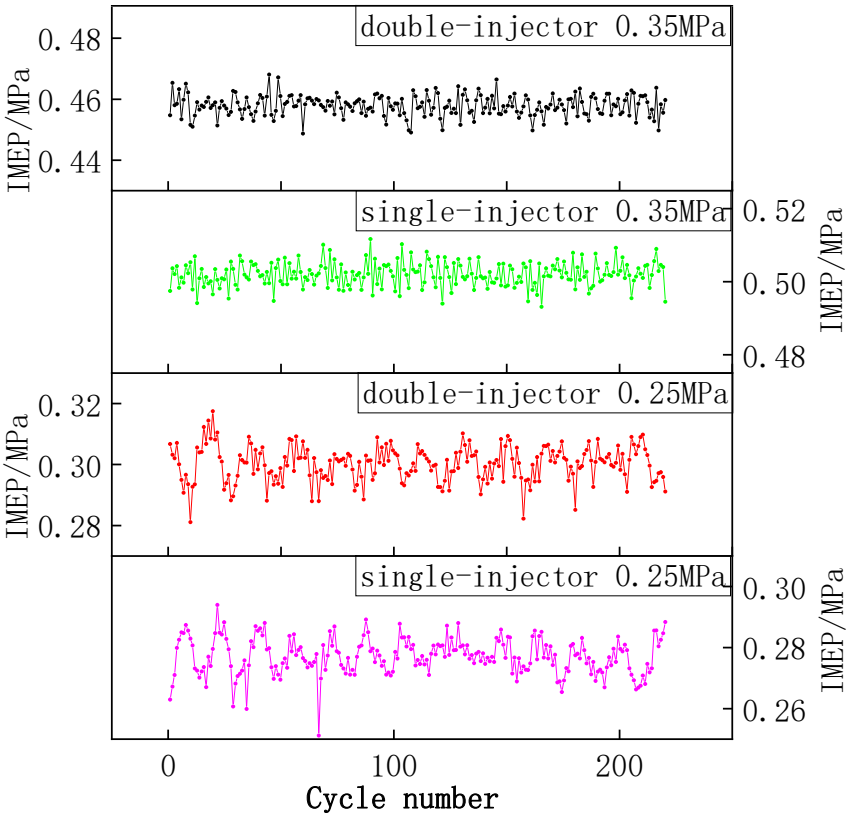

Figure 16. Comparison of IMEP for 220 Cycles at Different Loads.

The phenomenon can be explained by the following reasons. First, when the load is low, the mixture in the cylinder is lean and the flame propagation is affected, which will increase the CoV_{IMEP}. As the load increases, the mixture becomes richer and the combustion process is more stable, which can reduce the CoV_{IMEP}. Second, the hydrogen injection duration of the double-injector is shorter than the single-injector, and the mixing time of hydrogen and air is longer. Therefore, the mixture is more uniform, the combustion process is more stable, and the CoV_{IMEP} is smaller. Third, the use of the double-injector can alleviate the phenomenon of "blockage" in the intake manifold and reduce the residence time of hydrogen in the intake manifold. At the same time, it also can reduce the possibility of backfire and improve engine reliability. Furthermore, as described in Section 3.2, we know that the pressure rise rate and heat release rate in the cylinder of the single-injector

are larger, and the mechanical load and heat load of the engine are larger, which may also increase the abnormal combustion tendency and CoV_{IMEP} of the engine.

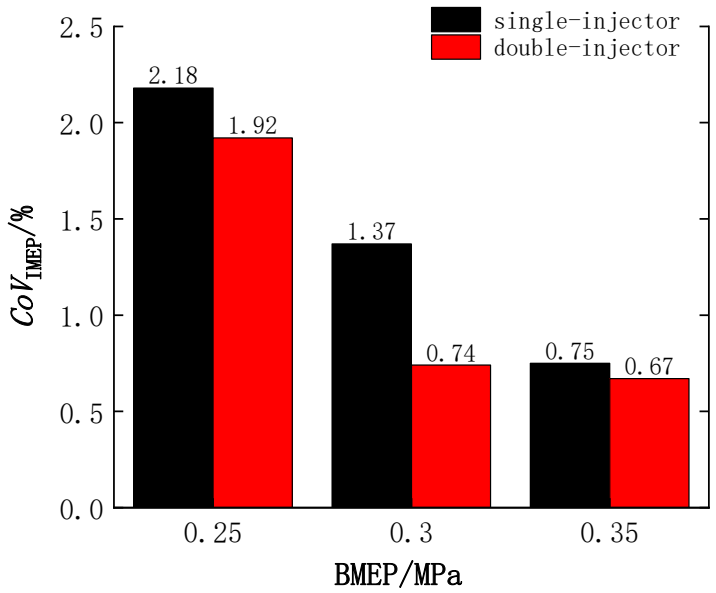

Figure 17. Comparison of the Coefficient of Variation of IMEP (CoV_{IMEP}) at Different Loads.

As shown in Figure 18, the effects of the single-injector and double-injector on the IMEP fluctuation at different speeds were comparatively studied. In Figure 19, the characteristic curve of CoV_{IMEP} concerning the engine speed is presented. The selected working condition is 2500~3500 rpm, the BMEP is 0.3 MPa, and the ignition timing is MBT ignition timing.

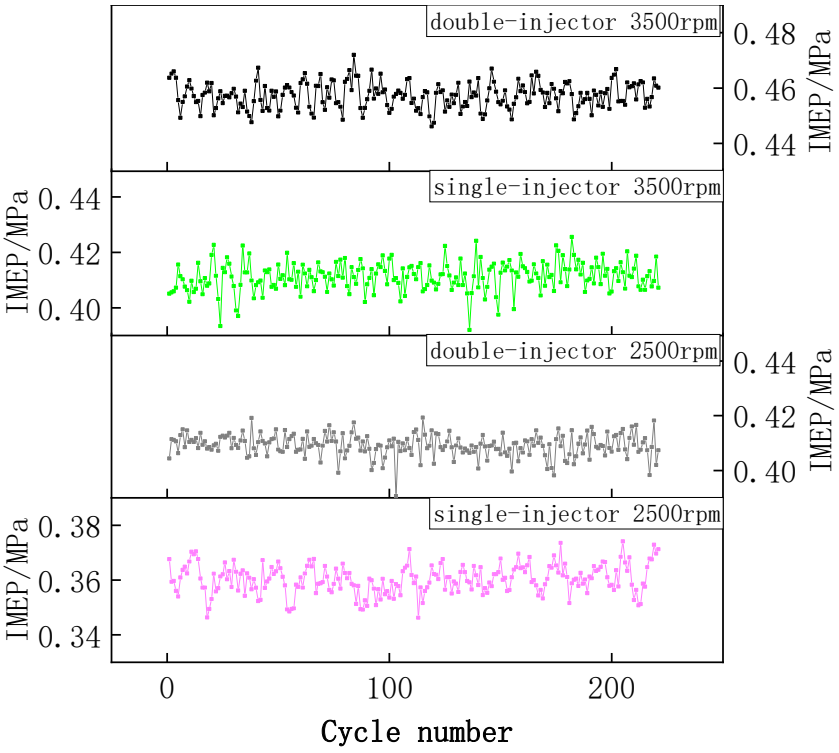

Figure 18. Comparison of IMEP for 220 Cycles at different engine speeds.

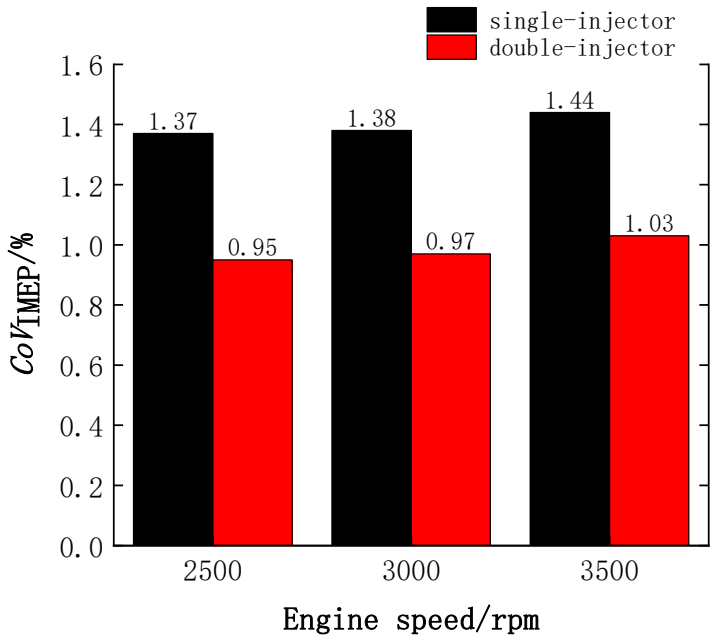

Figure 19. Comparison of CoV_{IMEP} at different engine speeds.

As shown in Figure 18, in the single-injector configuration, the IMEP fluctuation is greater than that of the double-injector. Figure 19 illustrates that the CoV_{IMEP} of the single-injector is greater than that of the double-injector. Because there is less pumping loss in the double-injector, it allows more fresh air to enter the cylinder. As a result, the scavenging efficiency is higher, which effectively reduces the cylinder temperature. Therefore, the CoV_{IMEP} of the double-injector is smaller. In addition, at low engine speeds, the CoV_{IMEP} is small. As the speed increases, there is a modest escalation in CoV_{IMEP}. This trend shows that the CoV_{IMEP} is not very sensitive to engine speed variations. This is because as the engine speed increases, the mixing time of hydrogen and air is greatly reduced, and the uniformity of the mixture in the cylinder deteriorates. Thus, the combustion process deteriorates and increases the CoV_{IMEP}. However, as the engine speed increases, the speed of airflow movement in the intake manifold is also increased, which can improve the mixing process of hydrogen and air and the combustion process, thereby reducing the large increase in CoV_{IMEP}.

4. Conclusions

Throughout the whole experimental investigation, the influences of single-injector and double-injector configurations on the performance and combustion characteristics of hydrogen internal combustion engines were scrutinized. Consequently, the ensuing conclusions are as follows:

(1) The injection capability of the single-injector is insufficient; the maximum power is 4.3 kW. Simultaneously, the in-cylinder mixture is lean, and the minimum excess air coefficient is 1.70. In contrast, the double-injector configuration has a superior injection capability, with a maximum power of 6.12 kW and a minimum excess air coefficient of 1.49. The double-injector configuration has significantly improved the engine performance, and the maximum power is increased by 42.3% compared with that of the single-injector configuration, which expands the performance boundary of the PFI hydrogen internal combustion engine.

(2) The double-injector can shorten the hydrogen injection duration and reduce the "blockage" of hydrogen in the intake manifold. At the same time, it increases the air intake of the engine, optimizes the scavenging process, and reduces the pumping losses. At a BMEP of 0.25 MPa, compared with that of the single-injector, the pumping loss of the double-injector is reduced from −0.049 MPa to −0.029 MPa.

(3) Under the same load conditions, compared with the single-injector, the maximum pressure rise rate of the double-injector is less than 0.098 MPa/°CA, and the maximum heat release rate is less than 22.82 J/°CA. It confirms that the combustion process of the double-injector configuration is relatively soft, which effectively reduces the mechanical load and thermal load of the engine and reduces the tendency of abnormal combustion.

(4) The highest indicated thermal efficiencies for the single-injector and double-injector configurations are 31.89% and 35.12%, respectively. Due to the high heat release rate, the heat transfer loss of the single-injector condition increases, so the thermal efficiency is lower.

(5) In the whole test working condition, the CoV_{IMEP} values of the single-injector and double-injector configurations are less than 2.18% and 1.92%, respectively. The double-injector configuration can reduce the CoV_{IMEP}. The double-injector shortens the duration of hydrogen injection and increases the mixing time of hydrogen and air, which makes the mixture in-cylinder more uniform. Therefore, the combustion is more stable and the CoV_{IMEP} is smaller.

With the intensification of global climate change and the energy crisis, countries around the world are looking for and researching clean energy. As a clean energy source, hydrogen has been proven to be used in internal combustion engines. For the transportation sector, the application of hydrogen internal combustion engines can achieve low carbon emissions. Therefore, hydrogen internal combustion engines are currently a research hotspot. In this study, the performance and combustion characteristics of a hydrogen internal combustion engine were studied by building an engine test bench. This will accelerate the practical application of hydrogen combustion engines, alleviate the fossil energy crisis, and promote global sustainability. More importantly, the object of this research is the hydrogen fuel internal combustion engine, which can be applied to small power systems in the near future after experimental studies. For the transportation industry, the application of hydrogen fuel internal combustion engines can significantly reduce the carbon emissions produced by traditional fossil fuels. At the same time, hydrogen is a green and renewable energy source, which is of great significance for creating a low-carbon and energy-saving society and promoting the sustainable development of society.

In summary, the double-injector configuration can reduce the CoV_{IMEP} of the hydrogen internal combustion engine while improving the performance boundary and thermal efficiency of the hydrogen internal combustion engine. This study explores the effect of the number of injectors on the performance of hydrogen internal combustion engines, filling a gap in this field. At the same time, in the real world, it also provides a practical way to optimize hydrogen combustion engines. For engines of different sizes, if two injectors can be installed, it should be possible to modify the intake manifold to a double-injector configuration.

Author Contributions: Conceptualization, L.B.; Methodology, S.Z., Q.L. (Qian Li) and W.D.; Software, X.T.; Validation, K.W.; Resources, B.S.; Data curation, Q.L. (Qinghe Luo); Writing—review & editing, M.H. All authors have read and agreed to the published version of the manuscript.

Funding: This research received no external funding.

Institutional Review Board Statement: Not applicable.

Informed Consent Statement: Not applicable.

Data Availability Statement: Data available on request due to privacy.

Conflicts of Interest: The authors Baigang Sun and Qinghe Luo were employed by the Beijing Institute of Technology and Beijing Institute of Technology Chongqing Innovation Center. The author Qian Li was employed by Chongqing Changan Automobile Co., Ltd. and Chongqing University. The authors Xuelin Tang and Wei Deng were employed by Chongqing Changan Automobile Co., Ltd. The remaining authors declare that the research was conducted in the absence of any commercial or financial relationships that could be construed as a potential conflict of interest.

Nomenclature

CoV_{IMEP}	coefficient of variation
PFI	port fuel injection
DI	direct injection
PMEP	pump mean effective pressure
BMEP	brake mean effective pressure
IMEP	indicated mean effective pressure
ITE	indicated thermal efficiency
λ	excess air coefficient
MBT	maximum brake torque

References

1. Qin, Z.; Bhattacharya, S.; Sharif, M.; Zhang, Z. Effects of Char and Volatiles Extraction on the Performance of Dual Bed Pyrolysis Gasification System. *Energy Fuels* **2019**, *33*, 4877–4889. [CrossRef]
2. Figaj, R. Energy and Economic Sustainability of a Small-Scale Hybrid Renewable Energy System Powered by Biogas, Solar Energy, and Wind. *Energies* **2024**, *17*, 706. [CrossRef]
3. Ahmadi, P.; Torabi, S.H.; Afsaneh, H.; Sadegheih, Y.; Ganjehsarabi, H.; Ashjaee, M. The effects of driving patterns and PEM fuel cell degradation on the lifecycle assessment of hydrogen fuel cell vehicles. *Int. J. Hydrogen Energy* **2020**, *45*, 3595–3608. [CrossRef]
4. Wu, X.; Fan, H.; Mao, Y.; Sharif, M.; Yu, Y.; Zhang, Z.; Liu, G. Systematic study of an energy efficient MEA-based electrochemical CO_2 capture process: From mechanism to practical application. *Appl. Energy* **2022**, *327*, 120014. [CrossRef]
5. Sharif, M.; Fan, H.; Sultan, S.; Yu, Y.; Zhang, T.; Wu, X.; Zhang, Z. Evaluation of CO_2 absorption and stripping process for primary and secondary amines. *Mol. Simul.* **2023**, *49*, 565–575. [CrossRef]
6. Wang, Z.; Shuai, S.; Li, Z.; Yu, W. A Review of Energy Loss Reduction Technologies for Internal Combustion Engines to Improve Brake Thermal Efficiency. *Energies* **2021**, *14*, 6656. [CrossRef]
7. Wang, X.; Wang, Y.; Bai, Y.; Wang, P.; Zhao, Y. An overview of physical and chemical features of diesel exhaust particles (Review). *J. Energy Inst.* **2019**, *92*, 1864–1888. [CrossRef]
8. Li, J. Charging Chinese future: The roadmap of China's policy for new energy automotive industry. *Int. J. Hydrogen Energy* **2020**, *45*, 11409–11423. [CrossRef]
9. Martín-Alcántara, A.; Pino, J.; Iranzo, A. New insights into the temperature-water transport-performance relationship in PEM fuel cells. *Int. J. Hydrogen Energy* **2023**, *48*, 13987–13999. [CrossRef]
10. Bartolucci, L.; Cennamo, E.; Cordiner, S.; Mulone, V.; Pasqualini, F.; Boot, M.A. Digital twin of a hydrogen Fuel Cell Hybrid Electric Vehicle: Effect of the control strategy on energy efficiency. *Int. J. Hydrogen Energy* **2022**, *48*, 20971–20985. [CrossRef]
11. Oliveri, L.; D'Urso, D.; Trapani, N.; Chiacchio, F. Electrifying Green Logistics: A Comparative Life Cycle Assessment of Electric and Internal Combustion Engine Vehicles. *Energies* **2023**, *16*, 7688. [CrossRef]
12. Sharif, M.; Wu, X.; Yu, Y.; Zhang, T.; Zhang, Z. Estimation of diffusivity and intermolecular interaction strength of secondary and tertiary amine for CO_2 absorption process by molecular dynamic simulation. *Mol. Simul.* **2022**, *48*, 484–494. [CrossRef]
13. Chen, G.; Wei, F.; Zhang, K.; Xiao, R.; Wang, Z.; Yang, S. Investigation on combustion characteristics and gas emissions of a high-pressure direct-injection natural gas engine at different combustion modes. *Energy Convers. Manag.* **2023**, *277*, 116617. [CrossRef]
14. Purayil, S.T.P.; Hamdan, M.O.; Al-Omari, S.A.B.; Selim, M.Y.E.; Elnajjar, E. Review of hydrogen–gasoline SI dual fuel engines: Engine performance and emission. *Energy Rep.* **2023**, *9*, 4547–4573. [CrossRef]
15. Chłopek, Z.; Sar, H.; Szczepański, K.; Zakrzewska, D. Operational Issues of Using Replacement Fuels to Power Internal Combustion Engines. *Energies* **2023**, *16*, 2643. [CrossRef]
16. Dhande, D.Y.; Sinaga, N.; Dahe, K.B. Study on combustion, performance and exhaust emissions of bioethanol-gasoline blended spark ignition engine. *Heliyon* **2021**, *7*, e06380. [CrossRef] [PubMed]
17. García, C.P.; Abril, S.O.; León, J.P. Analysis of performance, emissions, and lubrication in a spark-ignition engine fueled with hydrogen gas mixtures. *Heliyon* **2022**, *8*, e11353. [CrossRef] [PubMed]
18. Singh, R.; Altaee, A.; Gautam, S. Nanomaterials in the advancement of hydrogen energy storage. *Heliyon* **2020**, *6*, e04487. [CrossRef]
19. Bakar, R.A.; Kadirgama, K.; Ramasamy, D.; Yusaf, T.; Kamarulzaman, M.K.; Aslfattahi, N.; Samylingam, L.; Alwayzy, S.H. Experimental analysis on the performance, combustion/emission characteristics of a DI diesel engine using hydrogen in dual fuel mode. *Int. J. Hydrogen Energy* **2022**, *52*, 843–860. [CrossRef]
20. Balli, O.; Caliskan, H. Energy, exergy, environmental and sustainability assessments of jet and hydrogen fueled military turbojet engine. *Int. J. Hydrogen Energy* **2022**, *47*, 26728–26745. [CrossRef]
21. Falfari, S.; Cazzoli, G.; Mariani, V.; Bianchi, G.M. Hydrogen Application as a Fuel in Internal Combustion Engines. *Energies* **2023**, *16*, 2545. [CrossRef]
22. Aghahasani, M.; Gharehghani, A.; Mahmoudzadeh Andwari, A.; Mikulski, M.; Pesyridis, A.; Megaritis, T.; Könnö, J. Numerical Study on Hydrogen–Gasoline Dual-Fuel Spark Ignition Engine. *Processes* **2022**, *10*, 2249. [CrossRef]

23. Yang, J.; Meng, H.; Ji, C.; Wang, S. Comparatively investigating the leading and trailing spark plug on the hydrogen rotary engine. *Fuel* **2022**, *308*, 122005. [CrossRef]
24. Zareei, J.; Rohani, A.; Mazari, F.; Mikkhailova, M.V. Numerical investigation of the effect of two-step injection (direct and port injection) of hydrogen blending and natural gas on engine performance and exhaust gas emissions. *Energy* **2021**, *231*, 120957. [CrossRef]
25. Babayev, R.; Andersson, A.; Dalmau, A.S.; Im, H.G.; Johansson, B. Computational comparison of the conventional diesel and hydrogen direct-injection compression-ignition combustion engines. *Fuel* **2022**, *307*, 121909. [CrossRef]
26. Bao, L.Z.; Sun, B.G.; Luo, Q.H. Optimal control strategy of the turbocharged direct-injection hydrogen engine to achieve near-zero emissions with large power and high brake thermal efficiency. *Fuel* **2022**, *325*, 124913. [CrossRef]
27. Estrada, L.; Moreno, E.; Gonzalez-Quiroga, A.; Bula, A.; Duarte-Forero, J. Experimental assessment of performance and emissions for hydrogen-diesel dual fuel operation in a low displacement compression ignition engine. *Heliyon* **2022**, *8*, e09285. [CrossRef] [PubMed]
28. Cernat, A.; Pana, C.; Negurescu, N.; Nutu, C.; Fuiorescu, D.; Lazaroiu, G. Aspects of an experimental study of hydrogen use at automotive diesel engine. *Heliyon* **2023**, *9*, e13889. [CrossRef] [PubMed]
29. Gültekin, N.; Ciniviz, M. Experimental investigation of the effect of hydrogen ratio on engine performance and emissions in a compression ignition single cylinder engine with electronically controlled hydrogen-diesel dual fuel system. *Int. J. Hydrogen Energy* **2023**, *48*, 25984–25999. [CrossRef]
30. Tsujimura, T.; Suzuki, Y. Development of a large-sized direct injection hydrogen engine for a stationary power generator. *Int. J. Hydrogen Energy* **2019**, *44*, 11355–11369. [CrossRef]
31. Bayramoğlu, K.; Yılmaz, S. Emission and performance estimation in hydrogen injection strategies on diesel engines. *Int. J. Hydrogen Energy* **2021**, *46*, 29732–29744. [CrossRef]
32. Lalsangi, S.; Yaliwal, V.S.; Banapurmath, N.R.; Soudagar, M.E.M.; Balasubramanian, D.; Sonthalia, A.; Varuvel, E.G.; Wae-Hayee, M. Influence of hydrogen injection timing and duration on the combustion and emission characteristics of a diesel engine operating on dual fuel mode using biodiesel of dairy scum oil and producer gas. *Int. J. Hydrogen Energy* **2023**, *48*, 21313–21330. [CrossRef]
33. Liu, X.; Seberry, G.; Kook, S.; Chan, Q.N.; Hawkes, E.R. Direct injection of hydrogen main fuel and diesel pilot fuel in a retrofitted single-cylinder compression ignition engine. *Int. J. Hydrogen Energy* **2022**, *47*, 35864–35876. [CrossRef]
34. Liu, C.; Wang, Z.; Sun, M.; Wang, H.; Li, P.; Yu, J. Characteristics of the hydrogen jet combustion through multiport injector arrays in a scramjet combustor. *Int. J. Hydrogen Energy* **2018**, *43*, 23511–23522. [CrossRef]
35. Pu, C.; Guo, G.; Han, J.; Jiang, S. Effect of jet schemes of the double-nozzle strut injector on mixing efficiency of air and hydrogen for a scramjet combustor. *Int. J. Hydrogen Energy* **2022**, *47*, 22633–22649. [CrossRef]
36. Zareei, J.; Alvarez, J.R.N.; Albuerne, Y.L.; Gámez, M.R.; Linzan, Á.R.A. A Simulation Study of the Effect of HCNG Fuel and Injector Hole Number along with a Variation of Fuel Injection Pressure in a Gasoline Engine Converted from Port Injection to Direct Injection. *Processes* **2022**, *10*, 2389. [CrossRef]
37. Gao, J.; Wang, X.; Song, P.; Tian, G.; Ma, C. Review of the backfire occurrences and control strategies for port hydrogen injection internal combustion engines. *Fuel* **2022**, *307*, 121553. [CrossRef]
38. Wu, B. Numerical modeling of hydrogen mixing in a direct-injection engine fueled with gaseous hydrogen. *Fuel* **2023**, *341*, 127725. [CrossRef]
39. Yu, X.; Li, G.; Du, Y.; Guo, Z.; Shang, Z.; He, F.; Shen, Q.; Li, D.; Li, Y. A comparative study on effects of homogeneous or stratified hydrogen on combustion and emissions of a gasoline/hydrogen SI engine. *Int. J. Hydrogen Energy* **2019**, *44*, 25974–25984. [CrossRef]
40. Pandey, J.K.; Kumar, G.N. Study of combustion and emission of a SI engine at various CR fuelled with different ratios of biobutanol/hydrogen fuel. *Int. J. Hydrogen Energy* **2023**, *48*, 28222–28234. [CrossRef]